Proceedings Paper:
Afkhami, M, Hassanpour, A, Fairweather, M et al. (1 more author) (2014) Reynolds number effects on particle agglomeration in turbulent channel flow. In: Klemeš, JJ, Varbanov, PS and Liew, PY, (eds.) Computer Aided Chemical Engineering. 24th European Symposium on Computer Aided Process Engineering, 15-18 Jun 2014, Budapest, Hungary. Elsevier , 967 - 972. ISBN 978-0-444-63429-0

https://doi.org/10.1016/B978-0-444-63456-6.50162-9

Jiří Jaromír Klemeš, Petar Sabev Varbanov and Peng Yen Liew (Editors)
Proceedings of the 24th European Symposium on Computer Aided Process Engineering – ESCAPE 24
June 15-18, 2014, Budapest, Hungary.

Reynolds Number Effects on Particle Agglomeration in Turbulent Channel Flow

Mohammad Afkhami*, Ali Hassanpour, Michael Fairweather, Derrick O. Njobuenwu

Institute of Particle Science and Engineering, School of Process, Environmental and Materials Engineering, University of Leeds, Leeds LS2 9JT, UK
M.Afkhami5@leeds.ac.uk

Abstract

The work described in this paper employs large eddy simulation and a discrete element method to study particle-laden flows, including particle dispersion and agglomeration, in a horizontal channel. The particle-particle interaction model is based on the Hertz-Mindlin approach with Johnson-Kendall-Roberts cohesion to allow the simulation of Van der Waals forces in a dry air flow. The influence of different flow Reynolds numbers, and therefore the impact of turbulence, on particle agglomeration is investigated. The agglomeration rate is found to be strongly influenced by the flow Reynolds number, with most of the particle-particle interactions taking place at locations close to the channel walls, aided by the higher turbulence and concentration of particles in these regions.

Keywords: LES, DEM, particle, agglomeration, channel flow

1. Introduction

In this work, an advanced predictive technique for describing fluid motion, namely large eddy simulation (LES), is coupled with the discrete element method (DEM) to provide further understanding of flows containing solid particles. In the context of two- and multiphase horizontal channel flows, the most recent studies using one- and two-way coupled approaches for dispersed particle regimes are mainly focused on the influence of complex flow structures on particle motion, and the study of non-spherical particle shapes. Recent work on four-way coupled flows, considered herein, includes that of Alletto and Breuer (2012) who studied LES predictions of a particle-laden turbulent flow at high mass loading downstream of a confined bluff body. Mallouppas and van Wachem (2013) similarly used LES to study a turbulent particle-laden channel flow. These works however, did not consider particle agglomeration in the flow. It is worthy of note that direct numerical simulation (DNS) continues to be used to study such flows, although this is generally for low Reynolds number cases. Therefore one of the main challenges for LES is to compute flows with high precision at sufficiently high Reynolds numbers to more closely replicate those conditions found in practical applications. Furthermore, the dynamics of particle-laden fluid flows include a number of important aspects that dictate whether particle agglomeration will occur, affecting in turn particle dispersion and deposition. These include properties such as the instantaneous particle velocity, collision frequency and surface properties. As a result, many complications arise when analysing the underlying mechanisms responsible for agglomeration, and solving practical problems. The coupling of LES and DEM is an

effective approach that is capable of overcoming these issues, and providing insight as well as the potential to predict many practically-relevant flows.
The work described builds on previous findings presented at ESCAPE 23 (Afkhami et al., 2013) which used LES and DEM to demonstrate that a high particle mass loading is not required to promote particle agglomeration in turbulent channel flows.

2. Numerical Simulation

The LES employed a top-hat filter as this fits naturally into a finite-volume formulation. This decomposition is then applied to the Navier-Stokes equations for an incompressible Newtonian fluid with constant properties, bringing about terms which represent the effect of the sub-grid scale (SGS) motion on the resolved scale motions. The SGS stress model employed in this work was the dynamic model of Germano et al. (1996), applied using the approximate localisation procedure of Piomelli and Liu (1995). Computations were performed using the commercial CFD code ANSYS Fluent. The code implements an implicit finite-volume incompressible flow solver using a co-located variable storage arrangement. Because of this arrangement, a procedure similar to that outlined by Rhie and Chow (1983) is used to prevent checkerboarding of the pressure field. Time advancement is performed via an implicit method for all transport terms, and the overall procedure is second-order accurate in both space and time. The code is parallel and uses the message passing interface HP MPI. Further information on the mathematical model employed, and the numerical algorithm and its application, may be found in the ANSYS Fluent 13.0 theory guide.
A Lagrangian approach was used to model particle motion from the instantaneous fluid velocity field in which the particles are tracked along their trajectories through the unsteady, non-uniform flow field. The particle-laden flow was assumed to be dilute, and the method incorporated full coupling between the phases, i.e. interactions between particles were considered, and the flow and particles were two-way coupled. Particle-wall collisions were assumed to be inelastic. Particle-particle interactions were modelled using the discrete element method incorporating the contact model of Herz-Mindlin with Johnson-Kendall-Roberts cohesion (Johnson et al., 1971) to allow the simulation of the Van der Waals forces which influence particle behaviour. The particle surface attractive force was altered by specifying the surface energy. All particles were assumed to be soft spheres with equal diameter and density, and particles much heavier than the fluid were assumed. The effect of gravity was also neglected. Elghobashi and Truesdell (1993) have shown that the only significant forces in such systems are the Stokes drag and buoyancy forces, although buoyancy was also neglected in this work as the fluid was a gas. The shear induced Saffman lift force was taken into account as it assumes non-trivial magnitudes in the viscous sub-layer.
The flow is described by a three-dimensional Cartesian co-ordinate system (x, y and z) representing the streamwise, spanwise and wall-normal directions, respectively. The boundary conditions for the momentum equations were set to no-slip at the channel walls and the instantaneous flow field was considered to be periodic along the streamwise and spanwise directions, with a constant mass flux through the channel. The shear Reynolds numbers, $Re_\tau = hu_\tau/v$, used in the simulations were 150, 300 and 590 corresponding to bulk Reynolds numbers of $Re_b \sim 2100$, 4200 and 8260, respectively, based on half the channel height, h. The rectangular channel considered was of dimensions $2h \times 2\pi h \times 4\pi h$. The length of the channel in the streamwise direction was sufficiently long to capture the streamwise-elongated, near-wall turbulent structures that exist in wall-bounded shear flows. The non-uniform Cartesian grid used 1 million

computational nodes. The initial particle positions were distributed randomly throughout the channel, with their initial velocity set to 0 m s^{-1} and with the particles coming in-line with local flow velocities with time. Particles were assumed to interact with turbulent eddies over a certain period of time, that being the lesser of the eddy lifetime and the transition time. Particles that moved out of the channel were re-introduced into the computational domain using periodic boundary conditions. The total number of particles considered in the computational domain was 20,000 in all cases. Particle and fluid densities were set to $\rho_p = 1000$ and $\rho_f = 1.3$ kg m^{-3}, respectively, with the kinematic viscosity $v = 15.7 \times 10^{-6}$ m^2 s^{-1}. The particle relaxation time is given by $\tau_p = \rho_p d_p^2/18\rho U$, and the non-dimensional particle response time is defined as the particle Stokes number, $St = \tau_p^+ = \tau_p/\tau_f$, where τ_f is a characteristic time scale of the flow (defined as $\tau_f = v/u_\tau^2$, where the shear velocity $u_\tau = 0.221$). The particle surface energy considered was 0.5 J m^{-2}.

3. Results and Discussion

The results generated by the LES for the fluid phase were verified using DNS predictions for the various shear Reynolds number flows considered. Overall, the LES showed good agreement with the DNS, with the mean velocities and rms of fluctuating velocity components matching those of the DNS in both magnitude and position. The particle phase behaviour was also compared with one-way coupled DNS predictions, with results again in reasonable agreement with those derived on the basis of the DNS.

Figure 1 shows results for the number of particle bonds in the channel. The results clearly show an increase in the number of bonds with time due to the effects of flow turbulence on the particles; furthermore, the rate at which the particles form bonds increases with the flow Reynolds number. For all three shear Reynolds numbers, initially the rate of bond formation increases roughly linearly with time but then changes to a more exponential profile. In the higher shear Reynolds case, however, the trend is highly exponential, indicating an ever increasing rate at which particle bonds form with time. Further scrutiny of the results shows that agglomeration first occurs at approximately t = 0.001 s for the 300 and 590 Reynolds number flows; here the particles have increased their velocity to an extent where the flow turbulence now causes significant particle-particle interactions. In the case of the 150 Reynolds number flow, agglomeration is first seen at around t = 0.01 s, indicating a slower acceleration of the particles. A linear increase in particle bond numbers then continues to about t = 0.05 s, after which an increasing divergence is seen between the highest and lower Reynolds number flows. This trends is again repeated at t = 0.1 s where the $Re_\tau = 300$ flow deviates at an increasing rate from the $Re_\tau = 150$ case. This behaviour suggests that there is a mechanism within the flow that advantages the particles exposed to higher Reynolds numbers in the formation of agglomerates, other than the bulk flow velocity alone. This occurs as a result of regions of high particle concentration and low particle mean velocity near the channel walls; in such regions the number of bonds formed is proportionally higher for particles of higher Reynolds number as the particles migrate to these regions at a faster rate. Moreover, the increased shear in the high Reynolds number flows increases the intensity of these turbulent regions, and therefore the particle fluctuations and hence their interactions. Further analysis is required to establish a relationship between the particle fluctuating velocity and its impact on the formation of successful bonds. The dispersing behaviour of the particles and the regions in which bonds are formed are, however, discussed further below. At the end of the simulation, and for the $Re_\tau = 150$, 300 and 590 flows, respectively, there are 528, 635 and 1524 particle bonds in the flow. These figures further indicate that increases in flow Reynolds number dramatically enhance turbulence, and as a results particle agglomeration. It is thus clear that the effects of turbulence are significant in creating successful particle-particle bonds, and that the flow Reynolds number is a key factor in determining particle agglomeration

Figure 2 shows the time evolution of the number of particles close to the wall. The results clearly show that particles initially accumulate at the wall at an approximately linear rate. For Re_τ = 150, 300 and 590 particles are first seen to be in contact with the wall at 0.072, 0.055 and 0.037s, respectively. This behaviour suggests that the increasingly turbulent flow with increasing Reynolds number accelerates the particles at a faster rate in all directions (including towards the walls). From previous work, it is known that for turbulent channel flows particle positions close to a wall correlate with instantaneous regions of low velocity along the streamwise direction, with particles avoiding regions of high velocity. The behaviour observed in Figure 2 is also consistent with previous LES and DNS results where turbophoresis is known to cause the accumulation of particles in near-wall regions, which in the present flow also enhances the rate of particle agglomeration in such regions.

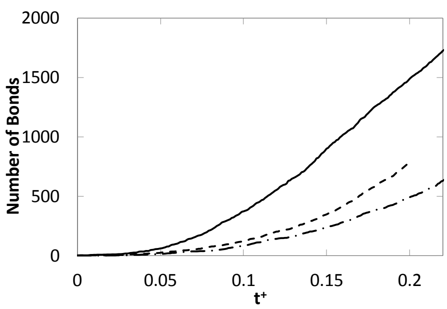

Figure 1: Number of bonds between particles with time (- · - ,- - - , — shear Reynolds numbers of 150, 300 and 590, respectively).

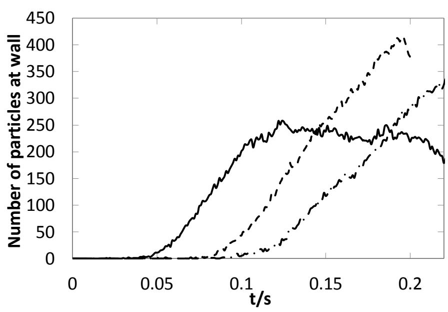

Figure 2: Particle number at the wall of the channel (- ·- ,- - - , — shear Reynolds numbers of 150, 300 and 590, respectively).

Figure 3 shows the location of particles with bonds in the wall-normal direction for all three Reynolds numbers, and their number at each location at time t = 0.2 s. Results are shown for 15 equally spaced regions across the channel, with particle statistics combined within each of the slabs of fluid considered. The columns for the number of bonds are plotted in relation to the channel walls, with columns 1 and 15 adjacent to the lower and upper walls, respectively. These two regions extend over the viscous sub-layer and buffer layer within the near-wall region. The results show a general movement of agglomerates towards the walls, indicated by columns 1 and 15 accounting for approximately 60% of the total particle bond count at all Re_τ. For Re_τ = 150, 300 and 590, at the channel centre (column 8) the number of bonds is 20, 18 and 47, respectively, with these values increasing towards the walls, where for columns 1 and 15 they increase to an average of 129, 203 and 249, respectively. Particle agglomeration near to the wall can be attributed to the high particle concentration and the high turbulence levels in this region (Afkhami et al., 2013).

Further scrutiny of the results shows that for the high Reynolds number flow, particle agglomeration is roughly double that of the other flows at the channel centre. This relationship also holds between the high and low Reynolds number flows at the channel walls, although the number of agglomerates at Re_τ = 300 is relatively closer to that of the Re_τ = 590 case. Such behaviour is indicative of higher turbulence in the Re_τ = 300 and 590 flows, which drives the particles to regions of lower fluid velocity. Throughout the flow, particle agglomeration is enhanced through high fluctuating velocities which affect a high number of particle-particle interactions, with peak levels typically at 30 wall units away from the solid boundaries. This influence is therefore most evident in the results for columns 2 and 14, which contain the highest agglomerate number, bar those regions closest to the walls where particle concentrations are high.

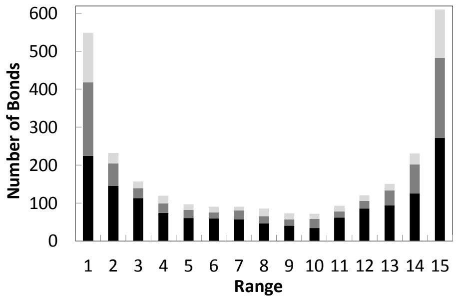

Figure 3: Agglomerate distribution across the channel (black – Re_τ = 590, mid-grey Re_τ = 300, light-grey Re_τ = 190).

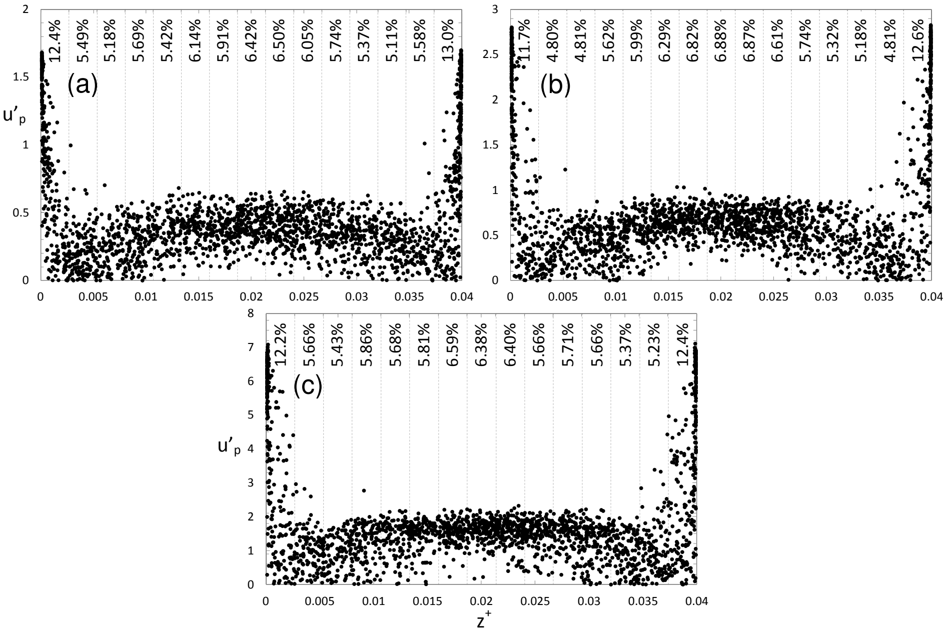

Figure 4: Instantaneous distribution of particle z^+ and u'_p for shear Reynolds numbers of (a) 150, (b) 300 and (c) 590 (t = 0.20s).

Lastly, Figure 4 gives the relationship between the instantaneous particle position in the wall-normal direction for all three Reynolds numbers, plotted against the particle fluctuating velocity magnitude in the streamwise direction at time t = 0.2s. The locations of the points are plotted relative to the lower wall. In general, the particles are well dispersed along the transverse direction, with more particles located close to the channel walls, as previously noted, where particle fluctuating velocities are higher than at other locations. In the regions closest to the walls, the particle velocity fluctuations show peak values of 1.7, 2.7 and 7.3 m s^{-1} with increasing Reynolds number, with particle proportion in these regions, on average, 12.7, 12.2 and 12.3%. These results clearly illustrate the dramatic increase in fluctuating velocities with Reynolds number in regions where preferential agglomeration occurs. In the next zones moving away from the walls, the peak fluctuating velocities are 1.2, 1.7 and 4.6 m s^{-1}, with average proportions of 5.5%, 4.8% and 5.5%, respectively. The range in particle velocity fluctuations in the highest Re_τ case demonstrates the significant influence of flow turbulence on particle agglomeration in both these regions. Relating the results of Figures 3 and 4, and the findings of Afkhami et al. (2013), the difference in particle agglomeration between the various Reynolds numbers in the latter zones can be attributed to a combination of both the particle mean velocity and the particle velocity fluctuation. Finally, at the channel centre, the particle velocity fluctuation peak values are 0.6, 1.1 and 2.1 ms^{-1}, for Re_τ = 150, 300 and 590. In this region the fluctuations are seen to be low, thereby explaining the lower levels of particle agglomeration.

4. Conclusions

Particles with identical physical parameters have been simulated in three channel flows with different levels of flow turbulence, achieved by increasing the Reynolds number of the flow, using a fully coupled LES-DEM approach. The particle size and surface energy selected were 150 µm and 0.5 J m^{-2}. Results derived for the three flows show that the rate of agglomeration is strongly influenced, and increases, with the intensity of the flow turbulence, with most of the particle-particle interactions taking place at locations close to the channel walls and in regions of high turbulence, where their agglomeration is aided both by the high levels of turbulence and the high concentration of particles. It can be concluded that it is a combination of the effect of both the flow mean and fluctuating velocities that is most significant in determining successful particle agglomeration in the channel flows considered.

References

M. Afkhami, A. Hassanpour, M. Fairweather, D.O. Njobuenwu, 2013, Particle-Interaction Effects in Turbulent Channel Flow, 23rd European Symposium on Computer Aided Process Engineering, Kraslawski, A., and Turunen, I. (Eds.), 847-852.

M. Alletto, M. Breuer, 2012, One-way, Two-way and Four-way Coupled LES Predictions of a Particle-laden Turbulent Flow at High Mass Loading Downstream of a Confined Bluff Body, Int. J. Multiphase Flow, 45, 70-90.

S. Elghobashi, G.C. Truesdell, 1993, On the Two-Way Interaction Between Homogeneous Turbulence and Dispersed Solid Particles, I: Turbulence Modification, Phys. Fluids A5, 1790-1801.

M. Germano, U. Piomelli, P. Moin, W.H. Cabot, 1996, Dynamic Subgrid-Scale Eddy Viscosity Model, In Summer Workshop, Center for Turbulence Research, Stanford, CA, 1996.

K.L. Johnson, K. Kendall, A.D. Roberts, 1971, Surface Energy and the Contact of Elastic Solids, Proc. R. Soc. A, 324, 301-313.

G. Mallouppas, B. van Wachem, 2013, Large Eddy Simulations of Turbulent Particle-Laden Channel Flow, Int. J. Multiphase Flow, 54, 65-75.

U. Piomelli, J. Liu, 1995, Large Eddy Simulation of Rotating Channel Flows Using a Localized Dynamic Model, Phys. Fluids, 7, 839-848.

C.M. Rhie, W.L Chow, 1983, Numerical Study of the Turbulence Flow Past an Airfoil with Trailing Edge Separation, AIAA J., 21, 525-532.